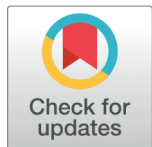


RESEARCH ARTICLE



Analyzing the Efficiency of Di-FeNPs in Removal of Methyl Orange Dye using Statistical Approach

OPEN ACCESS

Received: 29-03-2022

Accepted: 30-04-2022

Published: 09-06-2022

Yogita Sharma¹, Sunil Kumar², Rachna Bhateria^{2*}¹ Department of Environmental Science, ²Associate Professor, Department of Environmental Science, Maharshi Dayanand University, Rohtak, Haryana, India² Associate Professor, Department of Environmental Science, Maharshi Dayanand University, Rohtak, Haryana, India

Citation: Sharma Y, Kumar S, Bhateria R (2022) Analyzing the Efficiency of Di-FeNPs in Removal of Methyl Orange Dye using Statistical Approach. Indian Journal of Science and Technology 15(21): 1032-1040.

<https://doi.org/10.17485/IJST/v15i21.468>

* **Corresponding author.**

bioremediationlab.mdu@gmail.com

Funding: None

Competing Interests: None

Copyright: © 2022 Sharma et al. This is an open access article distributed under the terms of the [Creative Commons Attribution License](#), which permits unrestricted use, distribution, and reproduction in any medium, provided the original author and source are credited.

Published By Indian Society for Education and Environment ([iSee](#))

ISSN

Print: 0974-6846

Electronic: 0974-5645

Abstract

Objective: To study the catalytic potential of green synthesized iron nanoparticles for the removal of methyl orange dye. **Method:** Response Surface Methodology (RSM) was applied based on the Box-Behnken Design (BBD) which determined the interactive influence of parameters i.e., pH (1-3), adsorbent dose (80-120mg), initial dye concentration (5-15 ppm), contact time (60-90 minutes), and temperature (30-40°C) on methyl orange removal. **Findings:** BBD-RSM demonstrated that the Di-FeNPs achieved the maximum efficiency of 98% of methyl orange dye removal. In the present Model, F-value 214.94 implicates the significance of the model. The predicted R^2 of 0.9782 is closer to the adjusted R^2 of 0.989 which shows a good consistency among experimental and predicted values. The experimental data were analyzed by applying Redlich-Peterson ($R^2=0.982$), Elovich ($R^2=0.981$), and Dubinin-Radushkevich ($R^2=0.991$) isotherms models. **Novelty and applications:** The statistical approach using the Box-Behnken design indicates that this model is specific and accurate for the applied experimental data. Green synthesized iron nanoparticles have the potential to remove (98%) methyl orange dye.

Keywords: Iron nanoparticles; Methyl orange; Green synthesis; Response surface methodology; Datura innoxia; Isotherms

1 Introduction

Water pollution is created by the effluent released from several dye usage industries^(1,2). One of them is the textile industry which is water-intensive where water is used in various processes like dyeing and finishing. The effluent release by the textile industry comprises of toxic chemicals besides dye which is harmful for the living beings, aquatic. The colored water even loses its aesthetic value, and obstructs the penetration of sunlight which ultimately stops the photosynthesis reaction resulting in the death of aquatic plants⁽³⁾. Some treatment procedures for effluent discharged from textile industry have been used in the past such as advanced oxidation process, ion exchange, photodegradation, electrochemical degradation⁽⁴⁾ but have some limitations. Iron nanoparticles synthesized from Datura innoxia (Di-FeNPs) with their extraordinary

potential for adsorption, uniform size distribution, small size, and more surface area, are evidence to be an adsorbent leader to remove many pollutants specifically dyes from aquatic bodies⁽⁵⁾. The toxicity of products of chemical synthesis of metal NPs is a challenge in front of their absolute properties which have been resolved by the green synthesis procedures. Furthermore, to assess the potential of Di-FeNPs for methyl orange dye removal for optimization, this study was assisted with a statistical software Response Surface Methodology (RSM)⁽⁶⁾. RSM comprises a set of mathematical and statistical techniques to design experiments, and model building, to evaluate the relative significance of different independent variables and determines the optimum conditions for desired response. A primary limitation of RSM is that fitting data to a second order polynomial for systems that contain some curvature is often not well accommodated by the second order polynomials that are produced⁽⁷⁾. RSM reduces the number of experimental runs required to study the significance of parameters distressing the response of interest. Reghioua et al.,⁽⁸⁾ used RSM based on BBD for the optimization study of Remazol brilliant blue R dye removal using chitosan-glutaraldehyde/Fe₃O₄ composites incorporated with zinc oxide nanoparticles.

The aim of the present study is to synthesize iron nanoparticles (FeNPs) from leaves of *Datura innoxia* and to use these NPs for removal of methyl orange (MO) dye from synthetic dye solution. Various parameters affecting the removal of MO dye were optimized using batch mode⁽⁹⁾. For enhancing the removal efficiency of synthesized FeNPs, the interactive behaviors of various parameters such as pH, adsorbent dose (Di-FeNPs), initial dye concentration (MO), contact time, and temperature were studied using RSM-BBD (Design expert 11.0).

2 Methodology

2.1 Green synthesis of Di-FeNPs

To prepare leaf extract of *D. innoxia*, 5 g dried leaves were oven dried, powdered and boiled in 100 ml double distilled water for 15 minutes. The extract prepared was centrifuged at 2000 rpm⁽¹⁰⁾. FeNPs were synthesized by mixing ferric chloride (Ranbaxy Fine Chemicals Ltd. CAS: [7705-08-0]⁽⁹⁾) solution (0.10 M) with the leaf extract with further addition of NaOH. The FeNPs were separated from the solution through centrifugation at 15000 rpm. FeNPs were kept in an incubator at 35 °C^(11,12).

The batch studies done for optimization of MO dye removal were applied in RSM⁽¹²⁾. pH was set using HCl (0.1N) and NaOH (0.1N). The concentration of MO was measured by UV-visible spectrophotometer⁽¹³⁾.

3 Results and Discussion

3.1 Statistical analysis

The Box–Behnken experimental design combined with response surface modeling was employed⁽¹⁴⁾ for determining the effect of 5 parameters i.e., pH, adsorbent dose, initial dye concentration, contact time, and temperature on response i.e., removal of MO. In Table 1 the factor levels are mentioned. The predicted values are arranged in Table2.

Table 1. Factors and their low and high levels for Box Behnken Design

Factor	Parameters	Units	Range and levels		
			-1	0	+1
A	pH		1	2	3
B	Adsorbent dose	mg	80	100	120
C	Initial dye concentration	mg L ⁻¹	5	10	15
D	Contact time	minutes	60	75	90
E	Temperature	Degree Celsius	30	35	40

Table 2. Experimental and predicted response for Methyl orange dye removal using Box-Behnken Design matrix and response surface modeling

Runs	Experimental Factors					(% MO Adsorption)	
	A pH	B Adsorbent dose mg	C Initial dye concentration mg L ⁻¹	D Contact time minutes	E Temperature Degree Celsius	Response	Predicted

Continued on next page

Table 2 continued

1	1	100	10	60	35	86	83
2	2	100	5	75	40	92	91
3	3	100	10	90	35	48	50
4	2	120	10	90	35	96	95
5	2	100	10	75	35	97	96
6	1	100	10	90	35	88	87
7	3	100	10	60	35	43	42
8	2	80	5	75	35	85	85
9	2	100	15	75	40	90	89
10	1	100	15	75	35	88	86
11	2	100	10	60	30	85	84
12	3	120	10	75	35	50	50
13	2	120	15	75	35	92	92
14	2	80	10	90	35	84	84
15	2	100	10	75	35	96	96
16	3	100	15	75	35	48	47
17	1	80	10	75	35	82	81
18	2	100	10	75	35	97	96
19	3	100	5	75	35	49	48
20	2	100	10	75	35	98	96
21	1	100	10	75	40	84	85
22	2	100	10	90	40	93	92
23	3	100	10	75	30	43	44
24	2	80	10	60	35	82	81
25	2	100	15	60	35	85	87
26	2	120	5	75	35	92	92
27	2	100	15	75	30	90	89
28	1	100	5	75	35	88	86
29	2	100	5	60	35	84	86
30	2	80	15	75	35	84	84
31	1	120	10	75	35	85	87
32	2	100	10	75	35	95	96
33	3	80	10	75	35	44	40
34	2	100	10	60	40	86	85
35	2	100	10	90	30	91	90
36	2	100	5	90	35	94	93
37	2	100	5	75	30	90	88
38	2	80	10	75	40	83	83
39	2	80	10	75	30	82	82
40	3	100	10	75	40	47	48
41	2	120	10	75	40	94	92
42	2	120	10	60	35	88	86
43	2	100	10	75	35	98	96
44	2	120	10	75	30	92	90
45	2	100	15	90	35	93	92
46	1	100	10	75	30	84	85

Decolorization of MO (%) (Y) =	$96.83 - 19.56A + 3.93B - 0.25C + 3D + 0.75E + 0.75AB - 0.25AC + 0.75AD + 1AE + 0.25BC + 1.5BD + 0.25BE - 0.5CD - 0.5CE + 0.25DE - 26.66A^2 - 5.16B^2 - 2.75C^2 - 4.25D^2 - 4.25E^2$	Eq. 1
--------------------------------	--	-------

Equation 1 derived from the quadratic model reveals the relationship between independent and dependent variables. The magnitude of a variable signifies its intensity on response i.e., positive values signify a synergistic influence whereas negative indicates an antagonistic effect⁽¹⁵⁾. The variables such as pH (A), adsorbent dose (B), initial dye concentration (C) contact time (D), temperature (E), and their interactive influence AB, AD, AE, BC, BD, BE, and DE positively enhanced the reaction rate or removal efficiency with increase in variable level (equation 1). On the other hand, an increase in the intensity of variables with a

negative sign like A, C, AC, CD, CE, A², B², C², D² and E² decrease the rate of MO removal. Additionally, a higher value of the variables depicts their significance in dye removal for e.g., adsorbent dose (B) and contact time (D) are efficient variables over others. ANOVA was conducted to determine the relationship between the variable and their response based on the proposed model. The correlation coefficient (R² predicted, R² adjusted) specifies the quality of the fit for the regression model, and is expressed by correlating the experimental results with the response functions. Fischer’s-test was used to check the statistical importance⁽¹⁶⁾. Plots with three dimensions (3D) were drawn to assess the optimum conditions of response variables for MO removal. Table 3 shows the results of ANOVA using the model. Generally, lower values of probability (<0.05 is significant) <0.0001 and higher Fischer’s F statistics value (F=MS_{model}/MS_{error}), i.e., 214.94 implies model accuracy, means the quadratic polynomial model is significant for dye removal⁽¹⁷⁾. Moreover, a lack of fit of 0.1549 indicates that it is non-significant which is good for the model to fit. F-values of the parameters like pH (F-value 2042.11), adsorbent dose (F-value 82.73), and contact time (F-value 48.03) are more important factors in MO removal using Di-FeNPs than temperature. The interactive effect of adsorbent dose and contact time i.e., BD (F-value of 3.00) and pH and temperature (F-value of 1.33) are the most important interaction affecting the MO removal while other interactions show low F-values. The Predicted coefficient of determination i.e., R² of 0.9782 agrees with the adjusted R² which is 0.9896, only a 0.2 difference shows good consistency among predicted and experimental values. It specifies that the regression model better explains the relationship between the independent variables and their response⁽¹⁸⁾.

Table 3. Analysis of variance (ANOVA) for response surface quadratic model

Source	Sum of Squares	df	Mean Square	F-value	p-value	
Model	13018.23	20	650.91	214.94	< 0.0001	significant
A-pH	6123.06	1	6123.06	2021.92	< 0.0001	
B-Adsorbent dose	248.06	1	248.06	81.91	< 0.0001	
C-Initial dye concentration	1.0000	1	1.0000	0.3302	0.5707	
D-Contact time	144.00	1	144.00	47.55	< 0.0001	
E-Temperature	9.00	1	9.00	2.97	0.0971	
AB	2.25	1	2.25	0.7430	0.3969	
AC	0.2500	1	0.2500	0.0826	0.7762	
AD	2.25	1	2.25	0.7430	0.3969	
AE	4.00	1	4.00	1.32	0.2613	
BC	0.2500	1	0.2500	0.0826	0.7762	
BD	9.00	1	9.00	2.97	0.0971	
BE	0.2500	1	0.2500	0.0826	0.7762	
CD	1.0000	1	1.0000	0.3302	0.5707	
CE	1.0000	1	1.0000	0.3302	0.5707	
DE	0.2500	1	0.2500	0.0826	0.7762	
A ²	6206.06	1	6206.06	2049.33	< 0.0001	
B ²	232.97	1	232.97	76.93	< 0.0001	
C ²	66.00	1	66.00	21.79	< 0.0001	
D ²	157.64	1	157.64	52.05	< 0.0001	
E ²	157.64	1	157.64	52.05	< 0.0001	
Residual	75.71	25	3.03			
Lack of Fit	68.88	20	3.44	2.52	0.1549	not significant
Pure Error	6.83	5	1.37			
Cor Total	13093.93	45				

Df= degree of freedom

3.2 Optimization studies of parameters using 3D plots

Figure 1 shows the 3D plots, these plots demonstrate 3D interaction between the parameters in which the effect of two parameters plotted on the x-axis and y-axis and their effect/response are represented by the z-axis. Interaction between the

pH and adsorbent dose of the ternary solution and its effect or percentage removal of MO on the surface of Di-FeNPs is shown in Figure 1 a. From Figure 1 a, it can be concluded that as the pH increases to 3. This may be because the Di-FeNPs are reduced in less acidic conditions and a smaller number of hydroxyl ions are released which are responsible for initiating the catalytic oxidation reaction⁽¹⁹⁾. Adsorbent dose and pH are the most important parameters for adsorption studies⁽²⁰⁾. Figure 1 b depicts the interactive behavior of initial dye concentration and pH. Adsorption of 45% occurred at pH 3 and 15mg L⁻¹ initial dye concentration while adsorption increased to 96 % when pH got decreased to 2 and initial dye concentration of 10 mgL⁻¹. Figure 1 c shows the interactive effect of contact time along with pH. By increasing the contact time from 75 to 90 minutes, a decrease in MO dye adsorption was seen (88%) at pH 1. In Figure 1d at 30 °C 86% adsorption occurred but with an increase in temperature to 35 °C, an increase in adsorption (98%) was seen. Upon increasing the adsorbent dose from 100 mgL⁻¹ to 120 mgL⁻¹, the adsorption started decreasing to 93% at 5 mgL⁻¹ initial dye concentration which is presented in Figure 1e. In Figure 1f the interactive behavior of contact time and adsorbent dose can be seen on MO adsorption. With an increase in the adsorbent dose of 120 mgL⁻¹, the MO adsorption of 86% occurred at a contact time of 90minutes. Collective behavior of temperature and adsorbent dose was depicted in Figure 1 g. Here, 85% adsorption is achieved at 120 mg L⁻¹ adsorbent dose and a temperature 40° C. At contact time90 minutes and initial dye concentration15 mg L⁻¹, adsorption of 97% was observed (Figure 1 i). With the increase in temperature, adsorption got decreased (Figure 1 j). Likewise, an increase in contact time also leads to a decrease in the adsorption rate. As the temperature increased from 30°C to 40°C, a decrease in adsorption from 97°C to 90% was observed.

3.3 Adsorption isotherms

3.3.1 Redlich Peterson Isotherm Model

It is a 3-parameter empirical adsorption model and integrates features of the Langmuir and Freundlich isotherms and also corrects their inaccuracies. The linear form of the R–P equation is given as follows:

$$\ln C_e/q_e = \beta \ln C_e - \ln A$$

Redlich-Peterson isotherm models constants can be determined by simply plotting $\ln (C_e/q_e)$ against $\ln C_e$ (Figure 2 a), the slope is denoted by β (exponent, ranges from 0 to 1) and intercept by A (constant). When $\beta = 1$ R-P equation follows Langmuir adsorption isotherm. Likewise, R-P isotherm follows Freundlich adsorption isotherms when β becomes equal to 0. However, the accuracy of these interpretations strongly depends on the fitting method⁽²⁾.

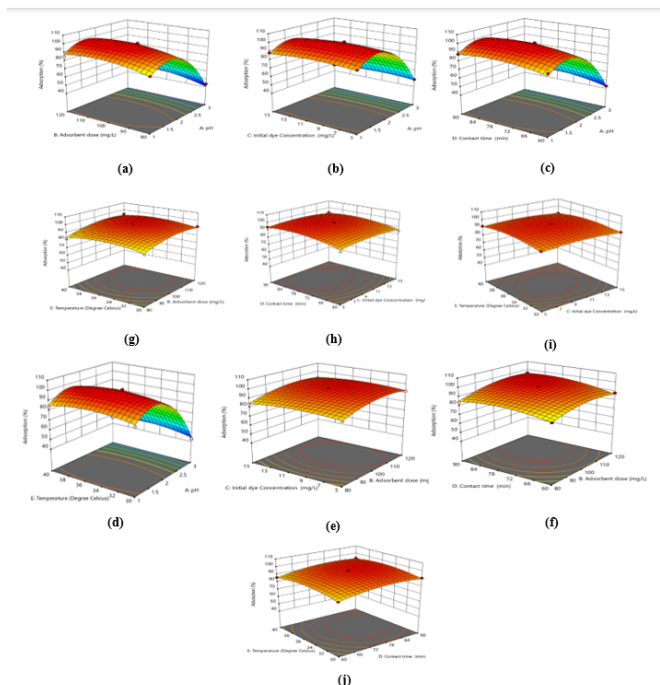


Fig 1. 3D plots showing interaction between (a) adsorbent dose and pH (b) initial dye concentration and pH (c) contact time and pH (d) temperature and pH (e) initial dye concentration and adsorbent dose (f) contact time and adsorbent dose (g) temperature and adsorbent dose (h) contact time and initial dye concentration (i) temperature and initial dye concentration and (j) temperature and contact time.

3.3.2 Elovich Isotherm

The Elovich model is useful in the prediction of mass and surface diffusion, activation, and deactivation energy of a system. The model assumes that the rate of adsorption of solute decreases exponentially as the amount of adsorbed solute gets increased⁽²¹⁾. The linear forms of the Elovich model is expressed as follows⁽²²⁾.

$$\ln \frac{q_e}{C_e} = \ln k_e q_m - q_e/q_m$$

Plotting a graph between $\ln (q_e/C_e)$ versus q_e (Figure 2b) gives Elovich's maximum adsorption capacity as well as Elovich's constant. The value for the coefficient of regression (R^2) for Elovich's isotherm is given in Table 6.

3.3.3 Dubinin and Raduskhevich isotherm (D-R isotherm)

To know the type of adsorption i.e., chemical and physical, D-R isotherm was analyzed. This model (Figure 2c) can be expressed as⁽²³⁾:

$$\ln q_e = \ln q_m - \beta \epsilon^2$$

here, q_e denotes the dye adsorbed per unit mass of adsorbent, q_m is the theoretical adsorption capacity, β is sorption energy constant, which is related to the average venegy of sorption per mole of the adsorbate as it is transferred to the surface of the solid from infinite distance in the solution, and ϵ is Polanyi potential, which is described as:

$$\epsilon = RT \ln \left(1 + \frac{1}{C_e} \right)$$

Where T denotes temperature (K) while R is gas constant. value of E (mean sorption energy) is given in table 6 derived from D-R parameter as follows:

$$E = \frac{1}{\sqrt{-2\beta}}$$

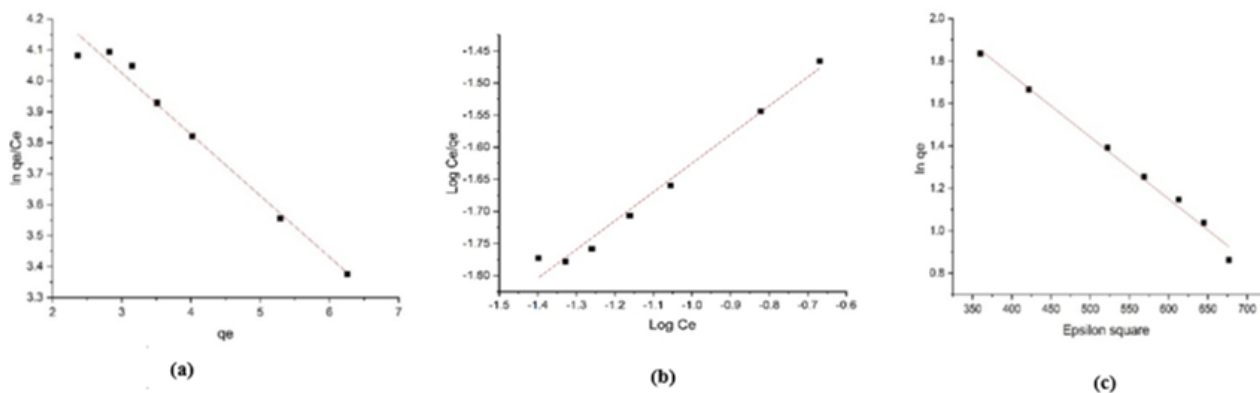


Fig 2. (a) Redlich Peterson isotherm (b) Elovich isotherm and (c) D-R Isotherm for methyl orange removal using Di-FeNPs

3.4 Multivariate Analysis

3.4.1 Principal component analysis

A biplot for principal component analysis was obtained using origin software version 2018 (Figure 3) representing the effect of parameters on adsorption eigenvalue, four principal components (PCs) were formed among them; two components (PC1 and PC 2) share 45.10 % of the cumulative variance. In PC 1, pH and initial dye concentration were negatively correlated with the PC i.e., adsorbent dose with the highest correlation value (0.137). However, other components (like temperature) have adsorbent dose. In PC 2, the contact time is the PC with PC is negatively correlated with both and adsorbent dose and positively correlated with pH and indicate the similarity of the patterns that represent these points⁽²⁴⁾

Table 4. Adsorption isotherm parameters and their values

Adsorption isotherm	Parameters	Values
D-R	qm	18
	K_{DR}	2.9×10^{-3}
	R^2	0.991
	β	0.447
R-P	A	15.03
	R^2	0.982
	qm	5.04
Elovich	Ke	2.49
	R^2	0.981

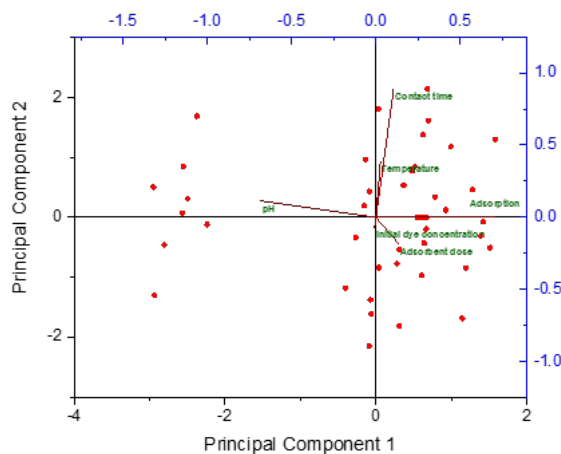


Fig 3. Principal component analysis (PCA) correlation (% variance) diagram of different variables for MO removal

Table 5. Correlation between variables and principal components

Parameters	Coefficients of PC1	Coefficients of PC2	Coefficients of PC3	Coefficients of PC4
pH	-0.68498	0.11486	0	0.22006
Adsorbent dose	0.13787	-0.1873	0.11331	0.95607
Initial dye concentration	-0.00875	-0.07049	0.04595	-0.0177
Contact time	0.10504	0.89143	-0.37465	0.18866
Temperature	0.02626	0.39	0.91907	-0.04008

3.4.2 Dendrogram

A tree structure called a dendrogram is commonly used to represent the process of hierarchical clustering. It shows how objects are grouped together (in an agglomerative method) or partitioned (in a divisive method)⁽²⁵⁾. The vertical axis of the dendrogram signifies the distance of dissimilarity among the clusters while the horizontal axis represents the clusters. In Figure 4, clusters are grouped as A, B, and C. The experimental runs performed B (1,7,34,29,25,11,2,19,28,5,15,18,20,32,43,23,46,37,10,16,27,9,21,40,36,45,35,36,22) are grouped under cluster A, runs performed under cluster B (8,17,33,39,30,38,24,14,4) while the cluster C includes groups (12,31,44,26,41,13,42). The clustering of the data is grouped according to their initial dye concentration. The clusters have been grouped on similarity of adsorbent dose given i.e., experimental runs under cluster A given a dose of 100 mg L⁻¹, cluster B 80 mg L⁻¹ and cluster C 120mg L⁻¹.

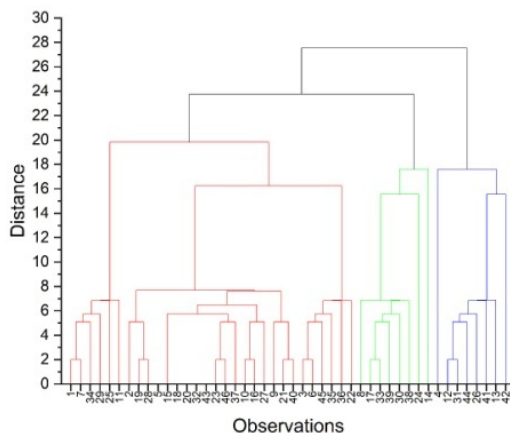


Fig 4. Dendrogram based on experimental data of methyl orange removal using Di-FeNPs

4 Discussion

The present study has been investigated to find an effective method for dye removal (methyl orange) using Di-FeNPs which is an eco-friendly approach. Response surface methodology based on box Behnken design was applied to 5 parameters. From the statistical studies, it has been concluded that the combinations of adsorbent dose and contact and also temperature and pH are the most effective combination for methyl orange dye removal. The closeness between the coefficient of determination shows a good relationship between experimental and predicted values. However, in principle component analysis also temperature and pH are the components that are positively correlated.

5 Conclusion

The obtained results given by BBD-RSM demonstrated that the Di-FeNPs achieved the maximum efficiency of 98% of methyl orange dye removal. F-values of pH (F-value 2042.11), adsorbent dose (F-value 82.73), and contact time (F-value 48.03) revealed to be important factors in MO removal. P- the value of <0.0001 of the model confirms that this design predicted the best optimum conditions for MO removal and fits well. R^2 value (adjusted) 0.98 and R^2 (predicted) 0.97 showed a good relationship between experimental and predicted values. The principal component is the adsorbent dose with the highest correlation value of 0.137 in the case of PC 1 while in PC 2, contact time is the principal component with a correlation value of 0.891. The principal component is negatively correlated with both initial dye concentration and adsorbent dose and positively correlated with pH and temperature. Among the three isotherms, D-R isotherm with a high value of correlation coefficient, i.e., R^2 0.99, was well suited for this study.

References

- 1) Jawad AH, Bardhan M, Islam MA, Islam MA, Syed-Hassan SSA, Surip SN, et al. Insights into the modeling, characterization and adsorption performance of mesoporous activated carbon from corn cob residue via microwave-assisted H₃PO₄ activation. *Surfaces and Interfaces*. 2020;21:100688–100688. Available from: <https://doi.org/10.1016/j.surfin.2020.100688>.
- 2) Chauhan M, Saini VK, Suthar S. Ti-pillared montmorillonite clay for adsorptive removal of amoxicillin, imipramine, diclofenac-sodium, and paracetamol from water. *Journal of Hazardous Materials*. 2020;399:122832–122832. Available from: <https://doi.org/10.1016/j.jhazmat.2020.122832>.
- 3) Jawad AH, Kadhum AM, Ngoh YS. Applicability of dragon fruit (*Hylocereus polyrhizus*) peels as low-cost biosorbent for adsorption of methylene blue from aqueous solution: kinetics, equilibrium and thermodynamics studies. *Desalination and Water Treatment*. 2018;109:231–240. doi:10.5004/dwt.2018.21976.
- 4) Jawad AH, Abdulhameed AS, Wilson LD, Syed-Hassan SSA, Alothman ZA, Khan MR. High surface area and mesoporous activated carbon from KOH-activated dragon fruit peels for methylene blue dye adsorption: Optimization and mechanism study. *Chinese Journal of Chemical Engineering*. 2021;32:281–290. Available from: <https://doi.org/10.1016/j.cjche.2020.09.070>.
- 5) Thacker H, Ram V, N D. Plant mediated synthesis of Iron nanoparticles and their Applications: A Review. *Progress in Chemical and Biochemical Research*. 2019;2(3):84–91. doi:10.33945/SAMI/pcbr.2019.183239.1033.
- 6) Jawad AH, Ishak MAM, Farhan AM, Ismail K. Response surface methodology approach for optimization of color removal and COD reduction of methylene blue using microwave-induced NaOH activated carbon from biomass waste. *Water Treatment*. 2017;62:208–220. doi:10.5004/dwt.2017.20132.

- 7) Bonaccorso A, Russo G, Pappalardo F, Carbone C, Puglisi G, Pignatello R, et al. Quality by design tools reducing the gap from bench to bedside for nanomedicine. *European Journal of Pharmaceutics and Biopharmaceutics*. 2021;169:144–155. Available from: <https://doi.org/10.1016/j.ejpb.2021.10.005>.
- 8) Reghioia A, Barkat D, Jawad AH, Abdulhameed AS, Rangabhashiyam S, Khan MR, et al. Magnetic Chitosan-Glutaraldehyde/Zinc Oxide/Fe₃O₄ Nanocomposite: Optimization and Adsorptive Mechanism of Remazol Brilliant Blue R Dye Removal. *Journal of Polymers and the Environment*. 2021;29(12):3932–3947. Available from: doi.org/10.1007/s10924-021-02160-z.
- 9) Abdulhameed AS, Mohammad ATT, Jawad AH. Modeling and mechanism of reactive orange 16 dye adsorption by chitosan-glyoxal/TiO₂ nanocomposite: application of response surface methodology. *DESALINATION AND WATER TREATMENT*. 2019;164:346–360. doi:10.5004/dwt.2019.24384.
- 10) Beheshtkhou N, Kouhbanani MAJ, Savardashtaki A, Amani AM, Taghizadeh S. Green synthesis of iron oxide nanoparticles by aqueous leaf extract of *Daphne mezereum* as a novel dye removing material. *Applied Physics A*. 2018;124(5):1–7. Available from: <https://doi.org/10.1007/s00339-018-1782-3>.
- 11) Shahwan T, Sirriah SA, Nairat M, Boyacı E, Eroğlu AE, Scott TB, et al. Green synthesis of iron nanoparticles and their application as a Fenton-like catalyst for the degradation of aqueous cationic and anionic dyes. *Chemical Engineering Journal*. 2011;172(1):258–266. Available from: <https://doi.org/10.1016/j.cej.2011.05.103>.
- 12) Sharma Y, Bhatia R. Phytoproduction of iron nanoparticles for methyl orange removal and its optimization studies. *Plant Archives*. 2021;21(no 1):939–954. Available from: <https://doi.org/10.51470/>.
- 13) Ghasemi SM, Ghaderpoori M, Moradi M, Taghavi M, Karimyan K. Application of Box-Behnken design for optimization of malachite green removal from aqueous solutions by modified barley straw. *Global NEST: the international Journal*. 2020;22(3):390–399. Available from: <https://doi.org/10.30955/gnj.003089>.
- 14) Mohammad ATT, Abdulhameed AS, Jawad AH. Box-Behnken design to optimize the synthesis of new crosslinked chitosan-glyoxal/TiO₂ nanocomposite: Methyl orange adsorption and mechanism studies. *International Journal of Biological Macromolecules*. 2019;129:98–109. Available from: <https://doi.org/10.1016/j.ijbiomac.2019.02.025>.
- 15) Lange K, Bruder A, Matthaai CD, Brodersen J, Paterson RA. Multiple-stressor effects on freshwater fish: Importance of taxonomy and life stage. *Fish and Fisheries*. 2018;19(6):974–983. doi:10.1111/faf.12305.
- 16) Ahmad A, Rehman MU, Wali AF, El-Serehy HA, Al-Misned FA, Maodaa SN, et al. Box-Behnken Response Surface Design of Polysaccharide Extraction from *Rhododendron arboreum* and the Evaluation of Its Antioxidant Potential. *Molecules*. 2020;25(17):3835–3835. doi:10.3390/molecules25173835.
- 17) Taha A, Da'na E, Hessien M. Evaluation of catalytic and adsorption activity of iron nanoparticles greenly prepared under different conditions: Box-Behnken design. *Molecular Simulation*. 2022;48(1):8–18. Available from: <https://doi.org/10.1080/08927022.2020.1784475>.
- 18) Boateng EY, Abaye DA. A Review of the Logistic Regression Model with Emphasis on Medical Research. *Journal of Data Analysis and Information Processing*. 2019;07(04):190–207. doi:10.4236/jdaip.2019.74012.
- 19) Xiang H, Ren G, Yang X, Xu D, Zhang Z, Wang X. A low-cost solvent-free method to synthesize α -Fe₂O₃ nanoparticles with applications to degrade methyl orange in photo-fenton system. *Ecotoxicology and Environmental Safety*. 2020;200:110744–110744. Available from: <https://doi.org/10.1016/j.ecoenv.2020.110744>.
- 20) Şahan T, Erol F, Yılmaz Ş. Mercury(II) adsorption by a novel adsorbent mercapto-modified bentonite using ICP-OES and use of response surface methodology for optimization. *Microchemical Journal*. 2018;138:360–368. Available from: <https://doi.org/10.1016/j.microc.2018.01.028>.
- 21) Kajjumba GW, Yıldırım E, Aydın S, Emik S, Ağun T, Osra F, et al. A facile polymerisation of magnetic coal to enhanced phosphate removal from solution. *Journal of Environmental Management*. 2019;247:356–362. Available from: <https://doi.org/10.1016/j.jenvman.2019.06.088>.
- 22) Riyanto CA, Prabalaras E. The adsorption kinetics and isotherm of activated carbon from Water Hyacinth Leaves (*Eichhornia crassipes*) on Co(II). *Journal of Physics: Conference Series*. 2019;1307(1):012002–012002. doi:10.1088/1742-6596/1307/1/012002.
- 23) Yeşilova E, Osman B, Kara A, Özer ET. Molecularly imprinted particle embedded composite cryogel for selective tetracycline adsorption. *Separation and Purification Technology*. 2018;200:155–163. Available from: <https://doi.org/10.1016/j.seppur.2018.02.002>.
- 24) Singh R, Bhatia R. Optimization and Experimental Design of the Pb²⁺ Adsorption Process on a Nano-Fe₃O₄-Based Adsorbent Using the Response Surface Methodology. *ACS Omega*. 2020;5(43):28305–28318. Available from: <https://doi.org/10.1021/acsomega.0c04284>.
- 25) Roux M. A Comparative Study of Divisive and Agglomerative Hierarchical Clustering Algorithms. *Journal of Classification*. 2018;35(2):345–366. doi:10.1007/s00357-018-9259-9.